Modeling European hot spells using extreme value analysis

Christiana Photiadou[1,2], Mari R. Jones[3,*], David Keellings[4], Candida F. Dewes[5]

[1]**Institute for Marine and Atmospheric Research Utrecht, Utrecht University, 3508 TA, Utrecht, The Netherlands**
[2]**Deltares, PO Box 177, 2600 MH, Delft, The Netherlands**
[3]**Earth System Laboratory, National Center for Atmospheric Research, Boulder, 80307-3000 Colorado, USA**
[4]**Department of Geography, University of Florida, Gainesville, 32611-7315 Florida, USA**
[5]**Department of Geography, UC Santa Barbara, Santa Barbara, 93106-4060 California, USA**

ABSTRACT: Atmospheric blocking in mainland Europe is often cited as the cause of extremely high temperatures lasting several days. By definition, extreme temperatures are rare, and yet the theory of extreme value statistics has seldom been applied to quantify the influence of atmospheric blocking on hot spells. Similarly, a comparison of the relative influence of other well-known atmospheric drivers, such as the North Atlantic Oscillation (NAO) and the El Niño-Southern Oscillation (ENSO), has seldom been explored. We applied a novel combination of extreme value and geometric distributions to observed daily temperature maxima from 74 stations across Europe, covering 1951–2010, to establish a stationary model of the expected magnitude, frequency and duration of hot spells that did not explicitly account for atmospheric drivers. Monthly time series of NAO, ENSO and 4 coherent atmospheric blocking regions were then incorporated as non-stationary covariates in the distribution parameter estimates to assess the dependence of hot spells on atmospheric covariates. We concluded that ENSO does not have a significant influence on hot spell magnitude or frequency; the NAO is a significant driver of hot spell magnitude (maximum attained temperature), frequency (annual event count) and duration (length of event) in northern Europe and Atlantic bordering stations; and atmospheric blocking is a significant driver of all aspects of hot spells in all parts of Europe. While NAO may increase peak temperatures by 2–4°C only in the north, relatively strong atmospheric blocking could result in increased temperatures of at least 4°C higher across Europe, with a commensurate increase in hot spell duration of 2–4 d.

KEY WORDS: Extreme value theory · Atmospheric blocking · NAO · North Atlantic Oscillation · ENSO · Europe

1. INTRODUCTION

The most visible impacts of global warming are manifested in local extreme temperatures, increasing the probability of extremely high temperatures (Katz & Brown 1992, Barriopedro et al. 2011, IPCC 2012, Mueller & Seneviratne 2012). Even considering the scarcity of extreme event data, it is very likely that daily temperature extremes are increasing with a commensurate reduction in the frequency of very cold days and nights and an increase in heat wave frequency and duration (IPCC 2012). Identifying and predicting the changing frequency of extreme high temperatures is problematic, but may be improved by combining statistical and physical approaches by including known atmospheric driving patterns in extreme value analyses (EVAs).

European temperature maxima are highly responsive to atmospheric circulation patterns (van Ulden & van Oldenborgh 2006), with large-scale synoptic pressure systems over a broad Atlantic domain (e.g. atmospheric blocking) influencing the occurrence

and distribution of extreme events such as hot spells (Haylock & Goodess 2004, Cassou et al. 2005). In particular, Europe has been identified as a region that experiences highly frequent and long-lasting blocking events (Woollings 2010). To better interpret, understand and predict changes in extreme temperature, it is important to quantify their dependence on often-cited causes such as atmospheric blocking, and compare this relationship with other atmospheric regimes such as the North Atlantic Oscillation (NAO) and the El Niño-Southern Oscillation (ENSO). Treating atmospheric blocking and NAO separately allows for an independent assessment of weather phenomena (e.g. atmospheric blocking) compared with large-scale climate variability (NAO) and, subsequently, the opportunity to improve the predictability of the proposed model under current climate conditions and for possible examinations of future climate scenarios.

Robust statistical tools are required to compare the relative influences of these atmospheric variables and to assess the likely impacts on the magnitude (maximum temperatures exceeding a specified threshold), frequency (annual count of maximum temperature excesses) and duration (number of continuous days of maximum temperature excesses) of hot spells. Trend analyses are only pertinent after the effects of climate variability have been accounted for (Kundzewicz & Robson 2004); by assessing the impacts of variable atmospheric processes on hot spells, their temporal evolution may be better diagnosed in future studies. For the purposes of this study we concentrated on the dependence of hot spells on atmospheric regimes rather than trends in the observational record.

EVA has been well established in the literature as a tool to investigate meteorological extremes (Katz et al. 2002). Scotto et al. (2011) analyzed the variability of observed European temperature extremes with EVA, finding distinct spatial differences. Brown et al. (2008) examined global daily maximum and minimum temperatures, using the NAO and a pre-determined linear trend in a non-stationary EVA, identifying significant increases in European maxima since 1950. Increases in daily temperature maxima and minima have been found using similar techniques in Spain (Cebrián & Abaurrea 2006), North America and continental Europe (Gershunov & Douville 2008, Unkašević & Tošić 2008), correlating the severity of temperature changes with driving atmospheric conditions. Sillmann et al. (2011) employed EVA to establish that the severity of European winter cold spells was significantly enhanced (i.e. colder) by atmospheric blocking. However, these studies were limited by a focus on the magnitude of daily temper-

ature minima and maxima, rather than a comprehensive examination of extreme temperature magnitude, frequency and duration.

Some have extended their analyses to use peak over threshold (POT) maxima to simulate droughts (Cebrián & Abaurrea 2006) or heat waves (Abaurrea & Cebrián 2002), making allowances for annual cycles, prevailing atmospheric conditions or trends with covariates (Katsoulis & Hatzianastassiou 2005). Furrer et al. (2010) extended the analysis further, developing a heat wave generator for summer daily maximum temperatures to analyze the frequency, magnitude and duration of temperature maxima exhibiting a strong temporal trend. Our analysis enhanced that approach with a larger selection of observation stations to analyze the spatial responses to atmospheric signals.

We were concerned with 3 large-scale circulation patterns that are known to influence European or global temperatures (Brönnimann et al. 2007): (1) ENSO; (2) the NAO, whose strong influence on the European winter climate is well known (Hurrell et al. 2003, Cassou et al. 2004) although its role in summer climate variability is not entirely understood (Jacobeit et al. 2009); and (3) atmospheric blocking. This article presents the development of a stationary model, premised on POT temperature maxima, to investigate the frequency, magnitude and duration of hot spells. The models were applied to a number of different stations throughout Europe to capture spatial differences in responses. We incorporated atmospheric variables into non-stationary distributions to investigate the relative changes in extreme temperature frequency, magnitude and duration with respect to atmospheric blocking, NAO and ENSO. A key novel component was the analysis of hot spell duration to ascertain the correlation between the atmospheric conditions and event longevity.

2. DATA

2.1. European Climate Assessment Dataset

Blended daily maximum temperature series were obtained from the European Climate Assessment Dataset (ECA&D) (Klein Tank et al. 2002) for 74 stations across Europe covering the period 1951–2010 (Fig. 1). Station observations were preferred over grid box average temperature series as the latter are known to have extreme temperatures up to 1°C lower than their observed counterparts (Zhang et al. 2011). Blended time series, which incorporate synoptic sta-
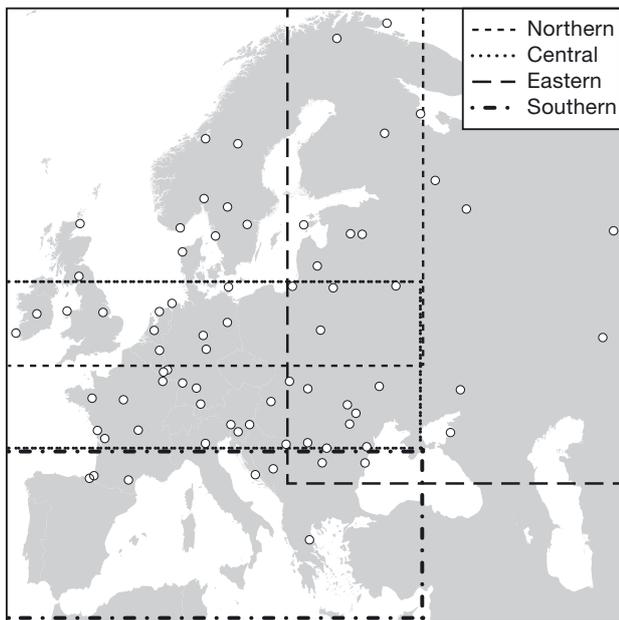
Fig. 1. Observation stations used in the analysis. Four atmospheric blocking regions are indicated by dotted and dashed lines: northern Europe, central Europe, southern Europe and eastern Europe

tion observations, were selected to minimize the number of missing observations; further information is provided in Klein Tank et al. (2002). Quality control rejected years with >3 missing days per month, >10 d within the summer season or stations with >5 yr missing over all. The homogeneity of temperature maxima was assessed for abrupt and gradual changes in the annual maxima to ensure that anthropogenic influences such as station re-location or urban heat island effects were not present, or could be incorporated in later analyses using the non-parametric Pettitt test (Pettitt 1979) for change points. No data inhomogeneities were identified in the daily maxima arising from anthropogenic influences.

2.2. Covariates

2.2.1. Atmospheric blocking

Atmospheric blocking events play a major role in the variability of the European climate through disruptions to prevailing cyclonic westerly flows by quasi-stationary high-pressure systems that can persist for a number of days (Schwierz et al. 2004). Summertime heat waves in the mid-latitudes are typically associated with persistent blocking anticyclones, and have a coherent spatial structure characterized by dry air and soil, no precipitation and increased fire

risk (Gershunov & Douville 2008). Together, these can create a positive feedback loop that perpetuates the hot spell.

Many European heat waves have arisen from atmospheric blocking conditions (Burt 2004, Dole et al. 2011, Grumm 2011). Links between meteorological responses along the periphery of the blocking regime are well known (e.g. Black et al. 2004). giving rise to extremes of temperature and precipitation such as the concurrence of the heat wave in Russia and floods in Pakistan during August 2010 (Weaver & Nigam 2008, Galarneau et al. 2012). Research has demonstrated that much of Europe, particularly Scandinavia and Russia, is climatologically disposed to heat waves arising from atmospheric blocking (Unkašević & Tošić 2008, Tyrlis & Hoskins 2008, Efthymiadis et al. 2011) .

Atmospheric blocking indices were obtained for the 4 main atmospheric response regions (illustrated in Fig. 1 with dotted and dashed lines), based on vertically averaged potential vorticity anomalies between the 500 and 150 hPa pressure layers (from ERA-40 data; Uppala et al. 2005). Negative potential vorticity anomalies (within regions) that lasted for at least 10 d were identified as blocking events (Sillmann & Croci-Maspoli 2009). The main advantage of the region-specific indices, rather than those calculated from averaged 500 hPa geopotential height (Tibaldi & Molteni 1990), is the ability to capture the dynamical features of the block. Further details of the theory and derivation of this blocking index can be found in Schwierz et al. (2004) and Croci-Maspoli et al. (2007).

2.2.2. NAO

The principal mode of variability in the north Atlantic, and in particular the European, sector weather patterns throughout the year, is the NAO, which is a dipole of mean sea level pressures (MSLP) between Iceland and the southern tip of the Iberian Peninsula (Jones & Conway 1997, Hurrell & Deser 2009). Indices of the NAO may be calculated either from the differences in surface pressure anomalies between the 2 locations, or from a principal component time series of the sea level pressures. Positive (negative) phases represent enhanced (diminished) Icelandic Low and Iberian High pressure fields. In its positive phase, warm moist air from enhanced westerly flows moves across Europe to generate dry conditions over southern Europe and North Africa, which influences drought persistence (Della-Marta et al. 2007). The summer NAO has been correlated

with droughts in the eastern Atlantic, Mediterranean and Sahel regions (Linderholm et al. 2009), while the winter (December to March) NAO is well established as a driver of precipitation in the north of Europe (Jones et al. 2003, Hurrell & Deser 2009).

A principal component analysis of the normalized MSLP differences between the Azores and Iceland has been shown to be more reliable for large spatial analyses due to the shifting center of action (Casty et al. 2005, Allan & Ansell 2006). Similarly, monthly values of the NAO index are considered to be more effective in explaining the occurrence of extreme weather patterns than their seasonal counterparts (Hurrell & Deser 2009, Jones et al. 2013). A monthly time series of the NAO index derived from principal component analysis over the Atlantic sector (20°–80° N, 90° W–40° E; Hurrell 1995) was obtained from the Climate Analysis Section of the National Center for Atmospheric Research. The monthly value corresponding with the occurrence of an extreme temperature was used to fit the non-stationary statistical model (see 'Fitting Statistical Models' below), while analyses of the impacts employed the maximum observed summertime value of the NAO index.

2.2.3. ENSO

Recent research has identified that ENSO can have a considerable influence on extreme European weather patterns (Trenberth et al. 2002, Brönnimann 2007), although very strong NAO years can modulate or mask European weather responses to ENSO (Zanchettin et al. 2008). Traditionally, Niño 3.4 is used as a measure of ENSO strength, but this index alone omits the connection with atmospheric processes, which are reflected through sea surface temperature (SST) anomalies. We selected the BEST index (Smith & Sardshmukh 2000), which is a combination of the atmospheric component, the Southern Oscillation Index (SOI) and the Niño 3.4 SST (averaged over the region 5° N–5° S, 170°–120° W), with the monthly mean climatology removed and a 3 mo running mean applied to the averaged SST and SOI series.

3. STATISTICAL THEORY

Extreme value theory provides an appropriate tool with which to analyze extreme temperature events, such as the frequency or magnitude of hot spells. Two principal methods are well established in the atmospheric sciences and hydrology literature: (1) modeling

excesses over a high threshold, or POT with a generalized Pareto distribution (GPD); and (2) modeling block maxima (such as the annual maximum temperature) with a generalized extreme value distribution (Coles 2001). A third approach that is now gaining popularity, initially developed from hydrological modeling for flood forecasting by Davison & Smith (1990), is to model the occurrence of the excesses and their magnitude jointly as a point process. Here we extend the statistical model further by incorporating atmospheric variables, and adding a geometric distribution to examine hot spell duration (Furrer et al. 2010).

3.1. Extended point process approach

For a series of extreme temperatures, such as temperature excesses over a high threshold, it is well established that independent and identically distributed data will conform to an extreme value distribution (Coles 2001). An advantage of the POT approach is that far more information about the upper tail of the distribution is available than would be possible with a smaller sample of the maximum value per year (AMAX). The magnitude of a series X of hot days exceeding a sufficiently high threshold, u, follows a GPD of the form:

$$H(x) = 1 - \left(1 + \frac{\xi_{GPD}(x-u)}{\tilde{\sigma}}\right)^{1/\xi_{GPD}} \tag{1}$$

with scale ($\tilde{\sigma}$) and shape (ξ_{GPD}) parameters, while their frequency are described by a Poisson distribution with exceedance rate λ. Selection of an appropriate threshold is often achieved through a stability exercise, where parameter estimates (and their standard errors) approximately stabilize. For consistency and ease of comparison, we adopted station-specific thresholds equivalent to the 95th quantile of the station daily temperature maxima (Q95); a quantile that achieved parameter stability for the majority of sites. While it is possible to vary the threshold in time, we were specifically interested in hot spells and did not consider a time-varying threshold to be appropriate.

The equivalent distribution for a sequence of block maxima, such as AMAX, is the generalized extreme value (GEV) distribution of the form:

$$G(x) = \exp\left[-\left(1 + \frac{(x-\mu)}{\sigma} \cdot \xi_{GEV}\right)^{-1/\xi_{GEV}}\right] \tag{2}$$

where μ is location, σ is scale and ξ_{GEV} is shape.

The point process relationship considers the occurrence and magnitude of the maxima as intrinsically related points in 2-dimensional space (Coles 2001).

As the count of POT maxima within a certain period (e.g. year) is equivalent to maxima arising from the GEV distribution over the same period, the parameters are directly related as (Davison & Smith 1990):

$$\xi_{GPD} = \xi_{GEV} = \xi$$
$$\tilde{\sigma} = \sigma + \xi(u - \mu) \qquad (3)$$
$$\lambda = \left[1 + \frac{\xi(u - \mu)}{\sigma}\right]^{-\frac{1}{\xi}}$$

Maximizing likelihood of the Poisson process yields estimates of the GEV parameters, from which the equivalent GPD and Poisson parameter estimates can be derived using Eq. (3); this facilitates interpretation of any covariates and the calculation of error terms (Davison & Smith 1990).

The assumption of independence is often violated by temperature maxima series, as these are often generated by the same weather system and can occur in clusters (Smith & Weissman 1985). Methods to identify independent sequences of POT temperature extremes range from simple approximations taking the maximum value of a sequence with a minimum interval between clustered extreme temperatures, to the use of complex models conditioned on the first excess in a sequence (Furrer et al. 2010). We adopted a minimum number of days with maximum temperature falling below *u* that was at least equal to the mean duration of the cluster of extremes (Ferro & Segers 2003) to define independent sequences of extremes.

3.1.1. Non-stationarity of extreme temperature distributions

While stationary models include some temporal variability through the use of all data over a period of time, the distribution parameter space is assumed to be constant for the period under consideration. However, extreme value distributions premised on stationarity are invalid in the presence of a strong seasonal pattern, atmospheric circulation patterns or anthropogenic changes (Cooley 2009). A commonly used approach to improve non-stationarity representation incorporates a generalized linear model (GLM) (Dobson 2002) into the statistical distribution parameter estimates. The simplest of these models introduces a linear trend term into the distribution parameters (e.g. Furrer et al. 2010), while more complex terms can also be built up to express trends through their dependence on highly variable atmospheric processes (Chavez-Demoulin & Davison 2005, Wood 2006).

Significant increases in European temperature minima and maxima are well reported (e.g. Unkašević & Tošić 2008, Della-Marta et al. 2009, Dole et al. 2011, Coumou & Rahmstorf 2012), and have been effectively used in non-stationary EVA to describe changes in extreme temperatures (Brown et al. 2008, Furrer et al. 2010). Our preliminary analyses of the POT daily maximum temperature series found no significant trends. Changes in the daily temperature minima or daily temperature range are often greater than those in the maxima (Christidis 2005, Unkašević & Tošić 2008, Brázdil et al. 2009, Donat & Alexander 2012), where heightened humidity may lead to enhanced cloud cover, suppressing the daily maxima while preventing night-time cooling (Gershunov et al. 2009), while natural variability may mask the presence of a weak trend if the magnitude of the variability exceeds that of the trend. Those studies that included trend terms in non-stationary extreme value distributions found that the models were improved by either the trend term or an atmospheric covariate, but not both. In the absence of a large sample of extreme temperatures from which to estimate trends, it is more appropriate to give credence to the atmospheric covariate information. Furthermore, we considered it more appropriate to include an implicit trend in the form of atmospheric circulation patterns rather than determine *a priori* the structure of a potentially non-linear trend.

We examined whether atmospheric patterns influence European hot spells by exploring improvements to the distribution fit using GLMs of atmospheric covariates, *y*, on the distribution parameters. The initial parameters can be described by:

$$\mu(\xi) = \beta_{0(1)} + \beta_{1(1)}Y$$
$$\ln[\sigma(x)] = \beta_{0(2)} + \beta_{1(2)}Y \qquad (4)$$
$$\xi(x) = \beta_{0(3)}$$

where $\beta_{0(i)}$ are the stationary model parameter estimates and $\beta_{1(i)}$ are linear transformations of the atmospheric covariates NAO, ENSO and blocking with respect to time. The shape parameter, ξ, was modeled as an intercept-only term with a constant, as this parameter is numerically difficult to estimate with any accuracy (Katz et al. 2002).

3.1.2. Hot spell duration

While the frequency and magnitude of temperatures exceeding a high threshold are well represented by the point process, 'spell' implies multiple days above the threshold. We defined a hot spell as a sequence of more than one day with temperatures exceeding *u*,

and examined the duration, z, using a geometric model with probability density function (P):

$$P(z) = p(1 - p)^{z-1} \quad \text{where} \quad z \geq 1 \quad (5)$$

where p is the reciprocal of the mean spell duration.

We adopted the discrete geometric distribution in preference to its continuous analogue, the exponential distribution, for its simplicity and ease of application (Wilks 2005). Non-stationarity in the time series and the influence of atmospheric patterns on hot spell duration were examined using a GLM of the distribution parameter estimates, where the geometric probability of a hot spell of duration of z days is governed by the stationary parameter estimates, $\beta_{0(i)}$, and linear transformations of the atmospheric covariates, $\beta_{1(i)}$.

$$p(z) = \beta_{0(4)} + \beta_{1(4)}Y \quad (6)$$

4. FITTING STATISTICAL MODELS

4.1. Stationary model

We applied stationary point processes to each station series of POT temperature maxima, assuming no time variance in the frequency and magnitude of hot spells; similar stationary models were developed with geometric distributions for hot spell duration. The suitability of the selected distributions was tested objectively through the use of quantile–quantile and probability distribution plots, examples of which are shown for Linköping, Sweden, in Fig. 2; parameter estimates are included in Table 1.

By definition, parameter estimates for the stationary model at 4 sites across Europe showed little spatial variation in the frequency of hot spells (λ) arising from the use of station-specific thresholds for a target quantile. For similar reasons, the geometric distribution parameter estimates (p) were largely the same across Europe, with mean hot spell durations of around 2 d. Estimates of the GEV location parameter (μ) reflected the climate at each station, with lower parameter values further north associated with lower air temperatures. Similarly, spatial variations in the scale parameter (σ) reflected the range of temperatures experienced at different locations, with those further from the sea or in larger landmasses having higher variability in the extreme temperatures than those in coastal locations. We found that most stations had a shape parameter (ξ) <0, likely arising from a physical upper bound on maximum temperatures (Furrer et al. 2010).

While the distributions were largely appropriate for lower tail maxima, it was also apparent that the most extreme maxima were not adequately represented. This is suggestive of either a secondary distribution for the highest extremes (Sornette 2009) or a controlling influence that exacerbates temperatures (Coumou & Rahmstorf 2012). Since atmospheric circulation patterns influence hot spells, and because there was an absence of sufficient extreme data to consider mixed distributions, we investigated improvements to the temperature representation by including covariates in the statistical models.

4.2. Non-stationary model

Several measures were employed to compare the non-stationary statistical models with the stationary
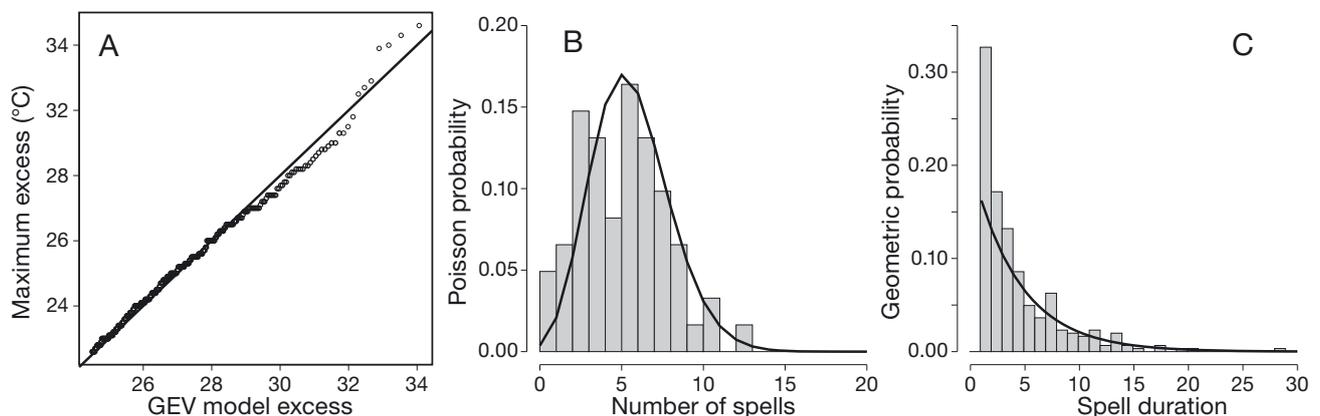

Fig. 2. Stationary model fits for: (A) temperature magnitude (generalized extreme value [GEV] distribution quantile–quantile plot); (B) peak over threshold frequency (Poisson probability distribution); and (C) hot spell duration (geometric probability distribution) for Linköping, Sweden

Table 1. Stationary model parameter estimates for μ: generalized extreme value location; σ: scale; ξ: shape; λ: Poisson rate; and 1/p: geometric mean; for 4 stations

Station	Location (μ)	Scale (σ)	Shape (ξ)	Mean hot spell frequency (λ)	Mean spell duration (1/p) (days)
Linköping, Sweden	28.80	2.01	−0.24	10.7	1.67
Orleans, France	33.35	1.99	−0.25	7.65	3.80
Larissa, Greece	40.04	1.96	−0.16	7.39	3.89
Smolensk, Russia	29.60	1.74	−0.16	7.00	4.20

models, as both subjective and objective measures are important to make an unbiased model selection (Villarini & Serinaldi 2011). Subjective measures included visual comparisons of quantile–quantile plots and fitted distribution functions; objective measures included the likelihood-ratio test, tested at the 5% significance level, or Akaike's information criterion (Akaike 1974). If N stations were temporally independent, 4 stations could be expected to accept the inclusion of a covariate incorrectly, as the distribution of field significant test results follows a binomial distribution of Bin ~ (N, α). However, temporal correlation between the stations, arising from a spatially extensive atmospheric signal, will result in overly optimistic confidence intervals. Karoly & Wu (2005) addressed this through a bootstrap resample of the field significance for gridbox squares, determining a spatial significance level of 19% for trends in surface temperatures with reference to the local significance level of 5% at each site. As resampling each 60-yr time series to improve the confidence interval estimates was computationally expensive, we made an allowance for temporal correlation by accepting field significance where the number of significant stations exceeded the nominal test level by at least 10% (Brown et al. 2008).

We compared the significance of each covariate separately for the GEV location and scale parameters, identifying whether temporal variability in either or both parameters improved the model fit. The significance of the atmospheric covariate in the statistical models is described below, and the resultant impact and implied direction of correlation (whether negative or positive) is described in Section 5. Increasing (decreasing) the location parameter would result in an increase (decrease) in the distribution mean; increasing the scale parameter increases the spread of the distribution with a higher density of the peak temperatures centered round the mean. Changes in these parameters are not explicitly examined in the following sections; rather, the overall impact on the distribution is presented. A full description of how changes in the

GEV parameters influence the overall distribution can be found in the Appendix.

4.3. Significance of covariates

4.3.1. GEV parameter estimates

Fig. 3 illustrates the significance of improvements to the GEV location and log-transformed scale parameters when ENSO and NAO were incorporated as covariate terms. ENSO improved the point process parameter estimates across the Central and Eastern Europe blocking regions (Fig. 3A,B), but the results were not field significant across the whole European domain. This demonstrates that although ENSO has a moderating influence on European extreme temperatures (Kenyon & Hegerl 2008), it is not a significant driver and instead enhances the effects of other atmospheric circulation patterns (Brönnimann 2007, Folland et al. 2009, Bladé et al. 2012). Therefore, we rejected ENSO as a covariate term in the point process model.

Although some have reported a positive correlation between hot spell intensity and summer NAO in eastern Europe (Unkašević & Tošić 2008, Efthymiadis et al. 2011), NAO was a significant covariate for the location parameter in north European stations (Fig. 3C,D); a statistically significant result at 30 stations also demonstrated field significance. In contrast, NAO was weakly negatively correlated with the scale parameter for all stations, but had no field significance. The resultant impact models incorporated NAO as a covariate only for the location parameter.

Atmospheric blocking was significantly correlated with both the GEV location and log-transformed scale parameters (Fig. 4). Each station was tested for its relative sensitivity to the blocking region, finding the greatest improvements to the statistical models for the blocking region covering the observation station; the influence of atmospheric blocking over regions far removed from the station was negligible
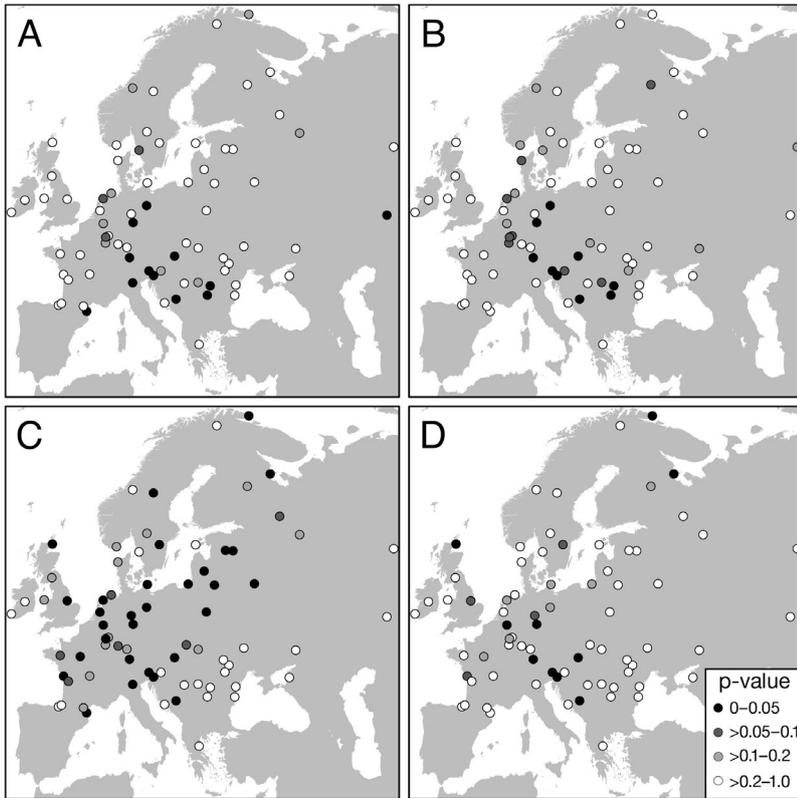
Fig. 3. Significance of improvements to the point process model for hot spell magnitude and frequency when including (A,B) the El Niño-Southern Oscillation and (C,D) the North Atlantic Oscillation as covariate terms. Significance: p ≤ 0.05. The covariates were introduced separately for the location (A,C) and scale (B,D) parameters

(e.g. Northern Europe blocking on south Europe temperatures). The location parameter was positively correlated with atmospheric blocking at stations in the north and negatively correlated in the south; in contrast, the scale parameter was negatively correlated with atmospheric blocking at all locations.

4.3.2. Geometric parameter estimates

Fig. 5 illustrates the significance of improvements to the geometric distribution when ENSO and NAO were incorporated as covariate terms. Contrary to the results for the GEV distribution, ENSO had a significant positive (negative) correlation with hot spell duration in northern and central (southern and eastern) Europe (Fig. 5A; for clarity, the direction of the correlation is not shown). Although the correlation with ENSO had field significance, our analysis was focused on all aspects of hot spells rather than a select feature such as event durations; in consequence, we did not use ENSO as a covariate in the impact models.

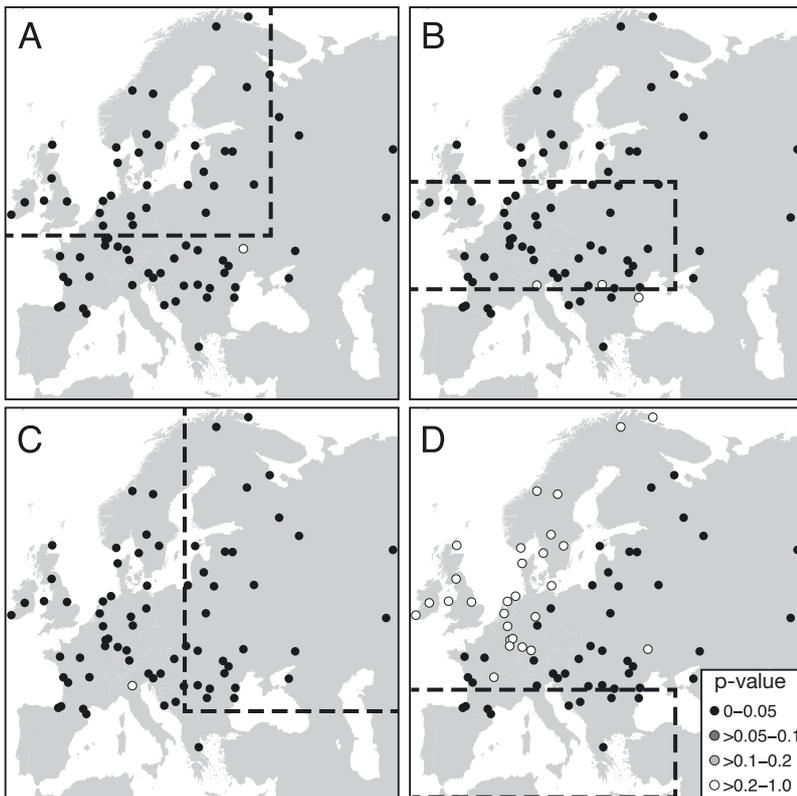The NAO had a significant influence on the duration of hot spells for

Fig. 4. Significance of improvements to the point process model for hot spell magnitude and frequency when including an atmospheric blocking index from the (A) northern, (B) central, (C) eastern and (D) southern regions (dashed lines). The covariates were introduced for both the location and scale parameters
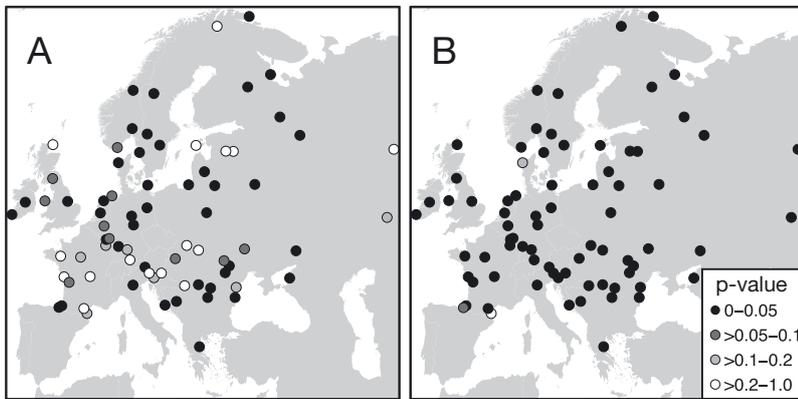
Fig. 5. Significance of improvements to the geometric distribution for hot spell duration when including covariate terms of (A) El Niño-Southern Oscillation and (B) North Atlantic Oscillation
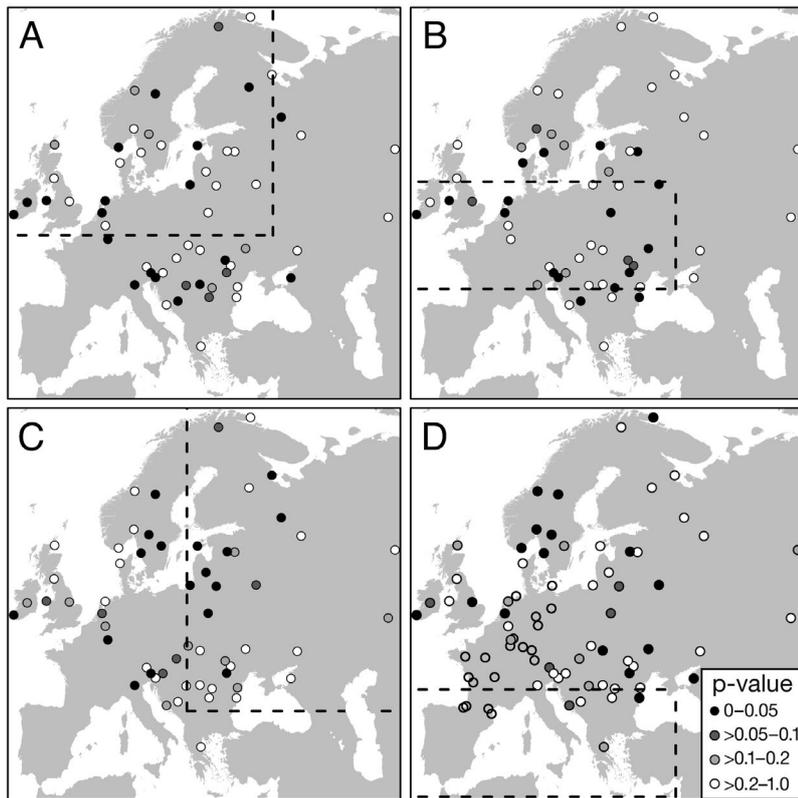

Fig. 6. Significance of improvements to the geometric distribution for hot spell duration when including an atmospheric blocking index from the (A) northern, (B) central, (C) eastern and (D) southern regions (dashed lines)

quency, it also increases the duration, while in other regions the NAO only has a secondary role influencing hot spells (Behera et al. 2012).

Fig. 6 illustrates the significance of improvements to the stationary geometric model using each of the 4 atmospheric blocking regions as covariates. The blocking region covering the observation station had the most significant relationship with hot spell duration; in all regions the direction of correlation was positive but is not illustrated for clarity. Atmospheric blocking over southern Europe had a very small degree of correlation, equivalent to no influence from atmospheric blocking. Others have also found that atmospheric blocking is not a significant influence on the occurrence of daily maximum temperatures in southern Europe (e.g. Katsoulis & Hatzianastassiou 2005, Carril et al. 2007), although it may influence the maximum night-time temperature in southwest Europe (Sanchez-Lorenzo et al. 2012).

5. ESTIMATED IMPACTS OF ATMOSPHERIC CIRCULATION

In this section we present the estimated impacts of atmospheric blocking and positive phases of the NAO on hot spell magnitude, frequency and duration at locations throughout Europe. To illustrate the likely degree of influence on the highest temperature maxima, we used the maximum observed value of June to August NAO and atmospheric blocking indices as covariates of the GEV and geometric parameters.

5.1. NAO

The influence of the NAO on hot spell magnitude, in absolute difference in degrees Celsius from the stationary model, is shown in Fig. 7 for the 10, 25 and 50 yr return period estimates (i.e. 10, 4 and 2% prob-

all of Europe, again with field significance (Fig. 5B). There was a statistically significant positive correlation between the NAO and hot spell duration in northern and western Europe and an insignificant negative correlation in the south and east. That is, in those regions where the NAO drives hot spell fre-
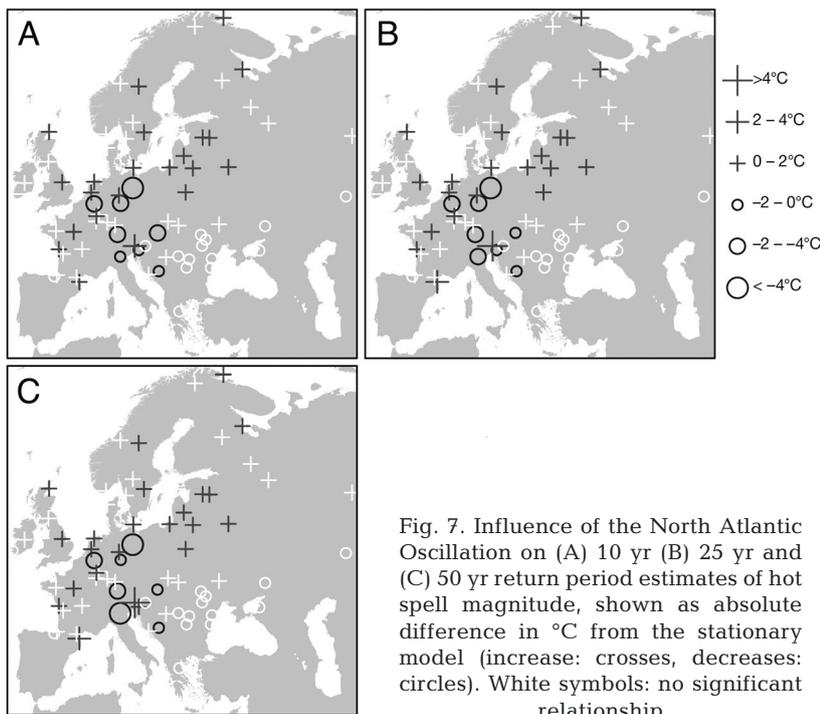
Fig. 7. Influence of the North Atlantic Oscillation on (A) 10 yr (B) 25 yr and (C) 50 yr return period estimates of hot spell magnitude, shown as absolute difference in °C from the stationary model (increase: crosses, decreases: circles). White symbols: no significant relationship

using the most significant regional blocking index as determined in 'Fitting Statistical Models'. Estimated temperature maxima show a widespread increase of between 2 and 4°C across Europe with the exception of a few stations. There is no specific spatial coherence in the stations reporting a decrease in event magnitude under the influence of atmospheric blocking, although elevation may be a factor (Scotto et al. 2011), as some stations in the Alps indicate the largest decreases of up to 4°C.

Fig. 10 shows the influence of atmospheric blocking on the estimated frequency and duration of hot spells, again using the station's proximate atmospheric blocking region. In an interesting contrast to the results presented both for the NAO and for northern Europe atmospheric blocking, many central and southern Europe stations report an increase (not always significant) in hot spell duration of 2 to 4 d, with a commensurate decrease in frequency. This is likely because an increase in the magnitude of temperature maxima, coupled with an increase in the duration of temperatures exceeding a high threshold, will result in fewer intervals between hot spells, and so apparently reduce their frequency.

ability of occurrence in any year). While data from a few stations in central Europe suggest that a highly positive phase of NAO decreases hot spell magnitude, the majority of stations that are influenced by the NAO report hot spell magnitudes of up to 2°C (an approximately 10% increase in magnitude in combination with the maximum value of NAO) during highly positive phases of the NAO.

Fig. 8 shows the influence of the NAO on hot spell frequency and duration, demonstrating that, in addition to increasing the magnitude of hot spells, positive phases of the NAO increase the frequency and duration. Under the influence of a highly positive phase of the summer NAO, there is an increased probability of hot spells in northern Europe with 2 to 4 more events; the probability decreases in central Europe and there is no change in the south. In contrast, and similar to the impacts reported for ENSO, NAO has a largely significant influence on the duration of hot spells in all parts of Europe, showing increases of 2 to 4 d.

6. CONCLUSIONS

We proposed a statistical model combining the point process and a geometric distribution to examine the effects of atmospheric blocking, the NAO and ENSO on the frequency, magnitude and duration of European hot spells. A POT approach identified the frequency and magnitude of extreme daily maximum temperatures, and the duration of the associated spell. Using known relationships between extreme value distribution parameters, we fitted the GEV distribution to the extracted maxima to simulate the frequency and magnitude of hot spells; with spell duration simulated from a geometric distribution. We then investigated the impacts of atmospheric non-stationarity on temperature maxima by combining the GEV and geometric parameter estimates with GLMs of covariates.

Our approach was implemented across a wide range of European stations, allowing a spatial repre-

5.2. Atmospheric blocking

Fig. 9 illustrates the influence of atmospheric blocking, in difference in degrees Celsius from the stationary model, for the 10, 25, and 50 yr return period temperature estimates. Results were calculated
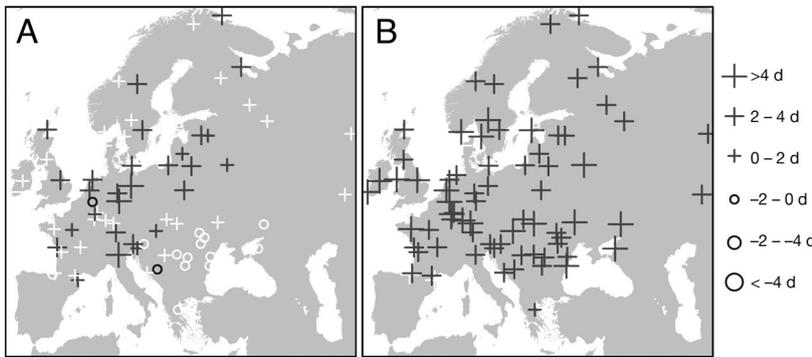
Fig. 8. Influence of the North Atlantic Oscillation on (A) frequency and (B) duration of hot spells shown as absolute differences in number of days between Poisson rate and geometric mean from the stationary model (increase: crosses, decreases: circles). White symbols: no significant relationship
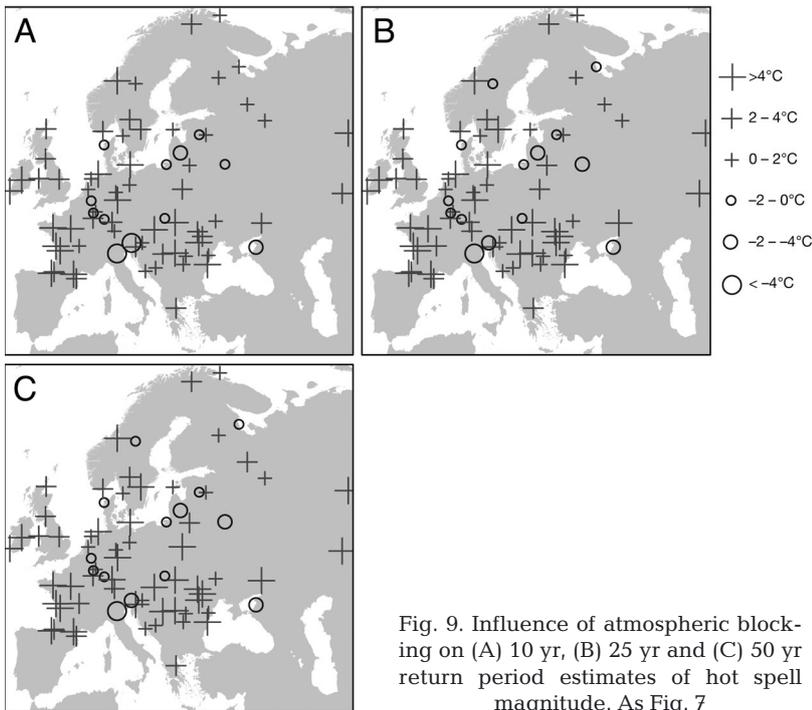

Fig. 9. Influence of atmospheric blocking on (A) 10 yr, (B) 25 yr and (C) 50 yr return period estimates of hot spell magnitude. As Fig. 7
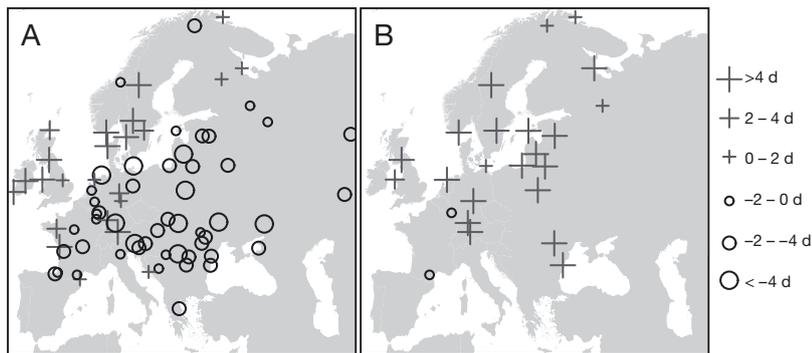

Fig. 10. Influence of atmospheric blocking on (A) frequency and (B) duration of hot spells. As Fig. 8

sentation of the influence of the co-variates. Using an extensive historical time series (1950–2010), we were able to establish meaningful connections between the different aspects of hot spells and large-scale circulations, which may be useful in estimating the likely future impacts of hot spells either for short-term forecasts or to assess longer-term impacts by downscaling future projections from climate models.

In agreement with others (Brönnimann 2007, Behera et al. 2012), we concluded that ENSO was not a significant driver of European hot spell frequency or magnitude; however, ENSO had a significant positive (negative) correlation with hot spell duration in northern and central (southern and eastern) Europe. NAO was a significant covariate only in the north and west of Europe, with positive correlations with the GEV location parameter and the geometric distribution. Again, this is supported by current research on the influence of the summer NAO over European meteorological events (Folland et al. 2009, Efthymiadis et al. 2011, Bladé et al. 2012). Atmospheric blocking was the most significant driver of hot spells in most of Europe, with the exception of the south, having a significant positive (negative) correlation with GEV location, and a significant positive (negative) correlation with the log-transformed scale in the northwest (southeast) of Europe.

The maximum recorded values of June to August NAO and atmospheric blocking over the period 1951–2010 were used to estimate their relative influences on hot spells. A highly positive phase of the summer NAO (such as June 1994) could increase temperature maxima by up to 2°C for the 10, 25 and 50 yr return periods in comparison to the stationary model, with a commensurate increase in the frequency and duration of hot spells in

northern Europe. However, in central and southern Europe, the same phase could result in a decrease in maximum temperatures of 0 to −4°C. In contrast, a strong atmospheric blocking event (e.g. July 2000) could result in maximum daily temperatures increasing by up to 4°C across Europe; this relationship appears to change with elevation, with stations in the Alps likely to experience lower temperatures of up to −4°C.

The statistical models used here assumed that increases in global mean temperature were effectively harnessed by the temporal variations in atmospheric circulation patterns. The benefit of assessing only the influence of atmospheric circulation patterns is that a better assessment of the immediate consequences of hot spell magnitude or duration can be made when a strong atmospheric blocking event is predicted, facilitating more realistic emergency planning. Further, the atmospheric-variable-driven approach has enabled greater understanding of the consequences of atmospheric blocking in different regions and of different phases of the NAO. This knowledge could be implemented in a hybrid statistical–dynamical downscaling approach with climate model output to improve estimates of the likely future changes in hot spell duration, magnitude or frequency.

While the incremental, and statistically negligible, changes in atmospheric circulation patterns may be adequately represented in this manner, the point process model dependent only on atmospheric blocking may not be appropriate for estimates of future changes in hot spells and may require an additional covariate term to represent trends (or abrupt changes) in the temperature maxima. This analysis used station observations to establish the statistical relationships with atmospheric drivers; the models would require validation against historical gridded temperature data prior to use with climate model output to ensure reasonable estimates of likely future temperature extremes.
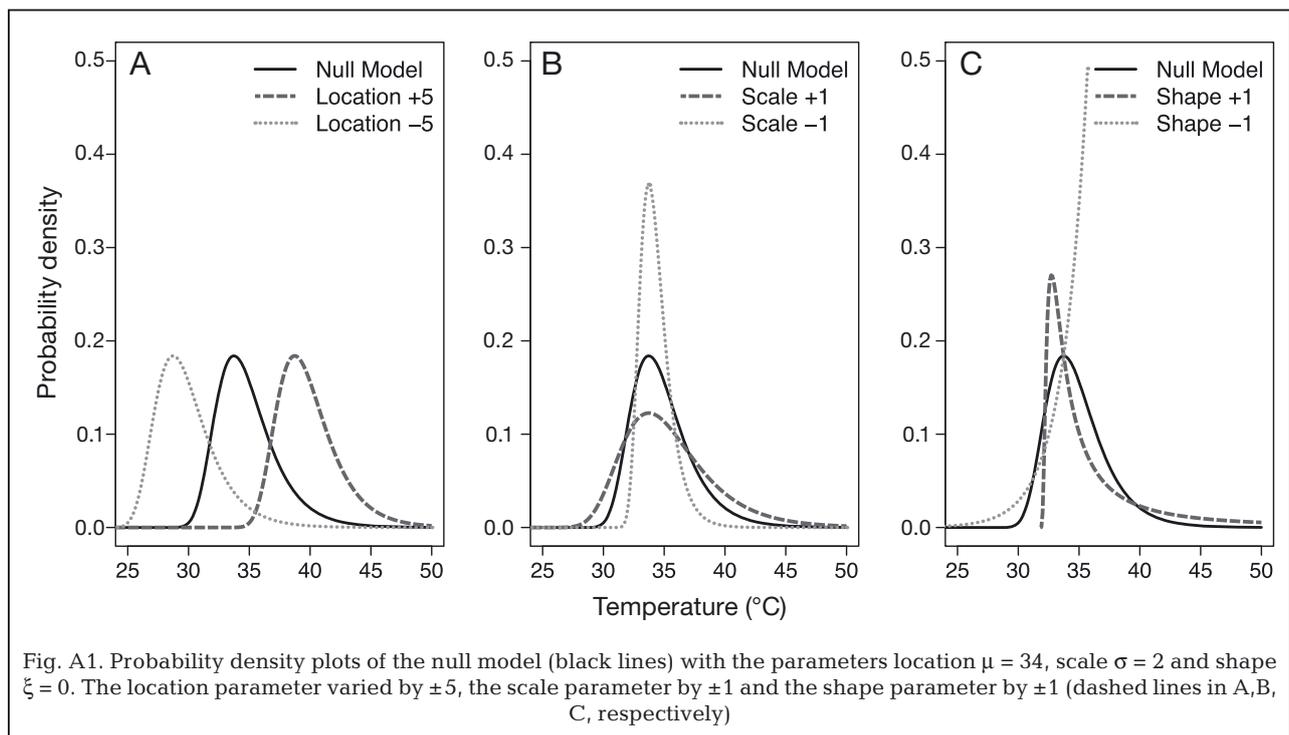
LITERATURE CITED

Abaurrea J, Cebrián AC (2002) Drought analysis based on a cluster Poisson model: distribution of the most severe drought. Clim Res 22:227–235

Akaike H (1974) A new look at the statistical model identification. IEEE Trans Automat Contr 19:716–723

Allan R, Ansell T (2006) A new globally complete monthly historical gridded mean sea level pressure dataset (Had-SLP2): 1850–2004. J Clim 19:5816–5842

Barriopedro D, Fischer EM, Luterbacher J, Trigo RM, García-Herrera R (2011) The hot summer of 2010: redrawing the temperature record map of Europe. Science 332:220–224

Behera S, Ratnam JV, Masumoto Y, Yamagata T (2012) Origin of extreme summers in Europe: the Indo-Pacific connection. Clim Dyn 41:663–676

Black E, Blackburn M, Harrison G, Hoskins B, Methven J (2004) Factors contributing to the summer 2003 European heatwave. Weather 59:217–223

Bladé I, Liebmann B, Fortuny D, van Oldenborgh GJ (2012) Observed and simulated impacts of the summer NAO in Europe: implications for projected drying in the Mediterranean region. Clim Dyn 38:1–19

Brázdil R, Chromá K, Dobrovolný P, Tolasz R (2009) Climate fluctuations in the Czech Republic during the period 1961–2005. Int J Climatol 29:223–242

Brönnimann S (2007) Impact of El Niño & Southern Oscillation on European climate. Rev Geophys 45:RG3003, doi: 10.1029/2006RG000199

Brönnimann S, Xoplaki E, Casty C, Pauling A, Luterbacher J (2007) ENSO influence on Europe during the last centuries. Clim Dyn 28:181–197

Brown SJ, Caesar J, Ferro CAT (2008) Global changes in extreme daily temperature since 1950. J Geophys Res 113:D05115, doi:10.1029/2006JD008091

Burt S (2004) The August 2003 heatwave in the United Kingdom. I. Maximum temperatures and historical precedents. Weather 59:199–208

Carril AF, Gualdi S, Cherchi A, Navarra A (2007) Heatwaves in Europe: areas of homogeneous variability and links with the regional to large-scale atmospheric and SSTs anomalies. Clim Dyn 30:77–98

Cassou C, Terray L, Hurrell JW, Deser C (2004) North Atlantic winter climate regimes: spatial asymmetry, stationarity with time, and oceanic forcing. J Clim 17: 1055–1068

Cassou C, Terray L, Phillips AS (2005) Tropical Atlantic influence on European heat waves. J Clim 18:2805–2811

Casty C, Wanner H, Luterbacher J, Esper J, Böhm R (2005) Temperature and precipitation variability in the European Alps since 1500. Int J Climatol 25:1855–1880

Cebrián AC, Abaurrea J (2006) Drought analysis based on a marked cluster Poisson model. J Hydrometeorol 7: 713–723

Chavez-Demoulin V, Davison C (2005) Generalized additive modelling of sample extremes. J R Stat Soc Ser C Appl Stat 54:207–222

Christidis N (2005) Detection of changes in temperature extremes during the second half of the 20th century. Geophys Res Lett 32:L20716, doi:10.1029/2005GL023885

Coles S (2001) An introduction to statistical modeling of extreme values. Springer-Verlag, Berlin

Cooley D (2009) Extreme value analysis and the study of climate change. Clim Change 97:77–83

Coumou D, Rahmstorf S (2012) A decade of weather

extremes. Nature Clim Change 2:1–6

Croci-Maspoli M, Schwierz C, Davies HC (2007) A multifaceted climatology of atmospheric blocking and its recent linear trend. J Clim 20:633–649

Davison AC, Smith RL (1990) Models for exceedances over high thresholds. J R Stat Soc, B 52:393–442

Della-Marta P, Luterbacher J, von Weissenfluh H, Xoplaki E, Brunet M, Wanner H (2007) Summer heat waves over western Europe 1880–2003, their relationship to large-scale forcings and predictability. Clim Dyn 29:251–275

Della-Marta PM, Mathis H, Frei C, Liniger MA, Kleinn J, Appenzeller C (2009) The return period of wind storms over Europe. Int J Climatol 29:437–459

Dobson AJ (2002) An introduction to generalized linear models. Chapman & Hall/CRC, Boca Raton, FL

Dole R, Hoerling M, Perlwitz J, Eischeid J and others (2011) Was there a basis for anticipating the 2010 Russian heat wave? Geophys Res Lett 38:L06702, doi:10.1029/2010 GL046582

Donat MG, Alexander LV (2012) The shifting probability distribution of global daytime and night-time temperatures. Geophys Res Lett 39:L14707, doi:10.1029/2012GL 052459

Efthymiadis D, Goodess CM, Jones PD (2011) Trends in Mediterranean gridded temperature extremes and large-scale circulation influences. Nat Hazards Earth Syst Sci 11:2199–2214

Ferro CAT, Segers J (2003) Inference for clusters of extreme values. J R Stat Soc Series B Stat Methodol 65:545–556

Folland CK, Knight J, Linderholm HW, Fereday D, Ineson S, Hurrell JW (2009) The summer North Atlantic Oscillation: past, present, and future. J Clim 22:1082–1103

Furrer EM, Katz RW, Walter MD, Furrer R (2010) Statistical modeling of hot spells and heat waves. Clim Res 43: 191–205

Galarneau TJJ, Hamill TM, Dole RM, Perlwitz J (2012) A multiscale analysis of the extreme weather events over Western Russia and Northern Pakistan during July 2010. Mon Weather Rev 140:1639–1664

Gershunov A, Douville H (2008) Extensive summer hot and cold extremes under current and possible future climatic conditions: Europe and North America. In: Diaz H, Murnane R (eds) Climate extremes and society. Cambridge University Press, Cambridge, p 74–98

Gershunov A, Cayan DR, Iacobellis SF (2009) The great 2006 heat wave over California and Nevada: signal of an increasing trend. J Clim 22:6181–6203

Grumm RH (2011) The Central European and Russian heat event of July–August 2010. Bull Am Meteorol Soc 92: 1285–1296

Haylock MR, Goodess CM (2004) Interannual variability of European extreme winter rainfall and links with mean large-scale circulation. Int J Climatol 24:759–776

Hurrell JW (1995) Decadal trends in the North Atlantic Oscillation: regional temperatures and precipitation. Science 269:676–679

Hurrell JW, Kushnir Y, Ottersen G, Visbeck M (2003) An overview of the North Atlantic oscillation. In: Hurrell JW, Kushnir Y, Ottersen G, Visbeck M (eds) The North Atlantic Oscillation: climate significance and environmental impact. Geophysical Monograph 134. American Geophysical Union, Washington, DC, p 1–35

Hurrell JW, Deser C (2009) North Atlantic climate variability: the role of the North Atlantic Oscillation. J Mar Syst 78:28–41

IPCC (2012) Managing the risks of extreme events and disasters to advance climate change adaptation. In: Field CB, Barros V, Stocker TF, Qin D and others (eds) A special Report of Working Groups I and II of the International Panel on Climate Change. Cambridge University Press, Cambridge

Jacobeit J, Rathmann J, Philipp A, Jones PD (2009) Central European precipitation and temperature extremes in relation to large-scale atmospheric circulation types. Meteorol Z 18:397–410

Jones PD, Conway D (1997) Precipitation in the British Isles: an analysis of area-averaged data updated to 1995. Int J Climatol 17:427–438

Jones PD, Osborn TJ, Briffa KR (2003) Pressure-based measures of the North Atlantic Oscillation (NAO): a comparison and an assessment of changes in the strength of the NAO and in its influence on surface climate parameters. In: Hurrell JW, Kushnir Y, Ottersen G, Visbeck M (eds) The North Atlantic Oscillation: climatic significance and environmental impact. Geophysical Monograph 134. American Geophysical Union, Washington, DC, p 51–62

Jones MR, Blenkinsop S, Fowler HJ, Stephenson DB, Kilsby CG 2013: generalized additive modelling of daily precipitation extremes and their climatic drivers. NCAR/TN-501+STR, http://nldr.library.ucar.edu/repository/assets/technotes/TECH-NOTE-000-000-000-868

Karoly DJ, Wu Q (2005) Detection of regional surface temperature trends. J Clim 18:4337–4343

Katsoulis BD, Hatzianastassiou N (2005) Analysis of hot spell characteristics in the Greek region. Clim Res 28:229–241

Katz RW, Brown BG (1992) Extreme events in a changing climate: variability is more important than averages. Clim Change 21:289–302

Katz RW, Parlange MB, Naveau P (2002) Statistics of extremes in hydrology. Adv Water Resour 25:1287–1304

Kenyon J, Hegerl GC (2008) Influence of modes of climate variability on global temperature extremes. J Clim 21: 3872–3889

Klein Tank AMG, Wijngaard JB, Können GP, Böhm R and others (2002) Daily dataset of 20th-century surface air temperature and precipitation series for the European Climate Assessment. Int J Climatol 22:1441–1453

Kundzewicz ZW, Robson AJ (2004) Change detection in hydrological records — a review of the methodology. Hydrol Sci J 49:7–19

Linderholm HW, Folland CK, Walther A (2009) A multicentury perspective on the summer North Atlantic Oscillation (SNAO) and drought in the eastern Atlantic Region. J Quaternary Sci 24:415–425

Mueller B, Seneviratne SI (2012) Hot days induced by precipitation deficits at the global scale. Proc Natl Acad Sci USA 109:12398–12403

Pettitt AN (1979) A non-parametric approach to the change-point problem. J R Stat Soc Ser C Appl Stat 28:126–135

Sanchez-Lorenzo A, Pereira P, Lopez-Bustins JA, Lolis CJ (2012) Summer night-time temperature trends on the Iberian Peninsula and their connection with large-scale atmospheric circulation patterns. Int J Climatol 32: 1326–1335

Schwierz C, Croci-Maspoli M, Davies HC (2004) Perspicacious indicators of atmospheric blocking. Geophys Res Lett 31:L06125, doi:10.1029/2003GL019341

Scotto MG, Barbosa SM, Alonso AM (2011) Extreme value and cluster analysis of European daily temperature series. J Appl Stat 38:2793–2804

Sillmann J, Croci-Maspoli M (2009) Present and future atmospheric blocking and its impact on European mean and extreme climate. Geophys Res Lett 36:L10702, doi: 10.1029/2009GL038259

Sillmann J, Croci-Maspoli M, Kallache M, Katz RW (2011) Extreme cold winter temperatures in Europe under the influence of North Atlantic atmospheric blocking. J Clim 24:5899–5913

Smith CA, Sardshmukh P (2000) The effect of ENSO on the intraseasonal variance of surface temperature in winter. Int J Climatol 20:1543–1557

Smith RL, Weissman I (1985) Maximum likelihood estimation of the lower tail of a probability distribution. J R Stat Soc B 47:285–298

Sornette D (2009) Dragon-kings, black swans and the prediction of crises. Int J Terraspace Sci Eng 2:1–18

Tibaldi S, Molteni F (1990) On the operational predictability of blocking. Tellus A Dyn Meteorol Oceanogr 42: 343–365

Trenberth KE, Caron JM, Stepaniak DP, Worley S (2002) Evolution of El Niño – Southern Oscillation and global atmospheric surface temperatures. J Geophys Res 107(D8), doi:10.1029/2000JD000298

Tyrlis E, Hoskins BJ (2008) Aspects of a Northern Hemisphere atmospheric blocking climatology. J Atmos Sci 65:1638–1652

Unkašević M, Tošić I (2008) Changes in extreme daily winter and summer temperatures in Belgrade. Theor Appl Climatol 95:27–38

Uppala SM, Kållberg PW, Simmons AJ, Andrae U and others (2005) The ERA-40 re-analysis. QJR Meteorol Soc 131: 2961–3012

van Ulden AP, van Oldenborgh GJ (2006) Large-scale atmospheric circulation biases and changes in global climate model simulations and their importance for climate change in Central Europe. Atmos Chem Phys 6:863–881

Villarini G, Serinaldi F (2011) Development of statistical models for at-site probabilistic seasonal rainfall forecast. Int J Climatol 32:2197–2212

Weaver SJ, Nigam S (2008) Variability of the Great Plains low-level jet: large-scale circulation context and hydroclimate impacts. J Clim 21:1532–1551

Wilks DS (2005) Statistical methods in the atmospheric sciences: an introduction. Academic Press, Burlington, MA

Wood SN (2006) Generalized additive models: an introduction with R. Chapman & Hall/CRC, Boca Raton, FL

Woollings T (2010) Dynamical influences on European climate: an uncertain future. Philos Trans R Soc Lond A 368:3733–3756

Zanchettin D, Franks SW, Traverso P, Tomasino M (2008) On ENSO impacts on European wintertime rainfalls and their modulation by the NAO and the Pacific multidecadal variability described through the PDO index. Int J Climatol 28:995–1006

Zhang X, Alexander L, Hegerl GC, Jones P and others (2011) Indices for monitoring changes in extremes based on daily temperature and precipitation data. Wiley Interdisciplinary Rev: Clim Change 2:851–870

Appendix. The following provides a brief exposition of the impact of changing the GEV parameters on the estimated temperature distributions. We fitted a nominal GEV distribution, broadly representing one of the stations in the Southern European region with the non-dimensional parameters location $\mu = 34$, scale $\sigma = 2$ and shape $\xi = 0$, here referred to as the null model. We then altered each parameter in turn, keeping the other 2 the same as the null model parameter, by a large enough percentage to visualize the change (these changes to the parameter estimates are not necessarily realistic)

Fig. A1. Probability density plots of the null model (black lines) with the parameters location $\mu = 34$, scale $\sigma = 2$ and shape $\xi = 0$. The location parameter varied by ±5, the scale parameter by ±1 and the shape parameter by ±1 (dashed lines in A,B, C, respectively)

Appendix (continued)

Fig. A1A shows that a change to the location parameter alone either increases or decreases the mean of the distribution, with no other changes to the distribution spread or skew. That is, it results in higher or lower temperature estimates for a given probability, as shown in Fig. A2A. Increasing (decreasing) the scale parameter affects the spread of the distribution, resulting in a commensurate increase (decrease) of the standard deviation about a constant mean, as shown in Fig. A1B. This translates into an increase (decrease) in the gradient of the return period estimate curve and, as such, much greater differences in maximum temperature estimates for higher return periods (i.e. lower annual probability). Finally, the shape parameter affects the skew of the distribution. An increase in the parameter to the upper limit of 1, shown in Fig. A1C, results in an upper bound distribution that is heavily left skewed, while decreasing the shape parameter to its lower limit of −1 results in a heavily right skewed distribution with an effective lower limit. Increases to the scale parameter translate into a downward curve and gradual change in the return period estimates, while decreases in the parameter result in a rapid increase in the maximum temperature estimates.
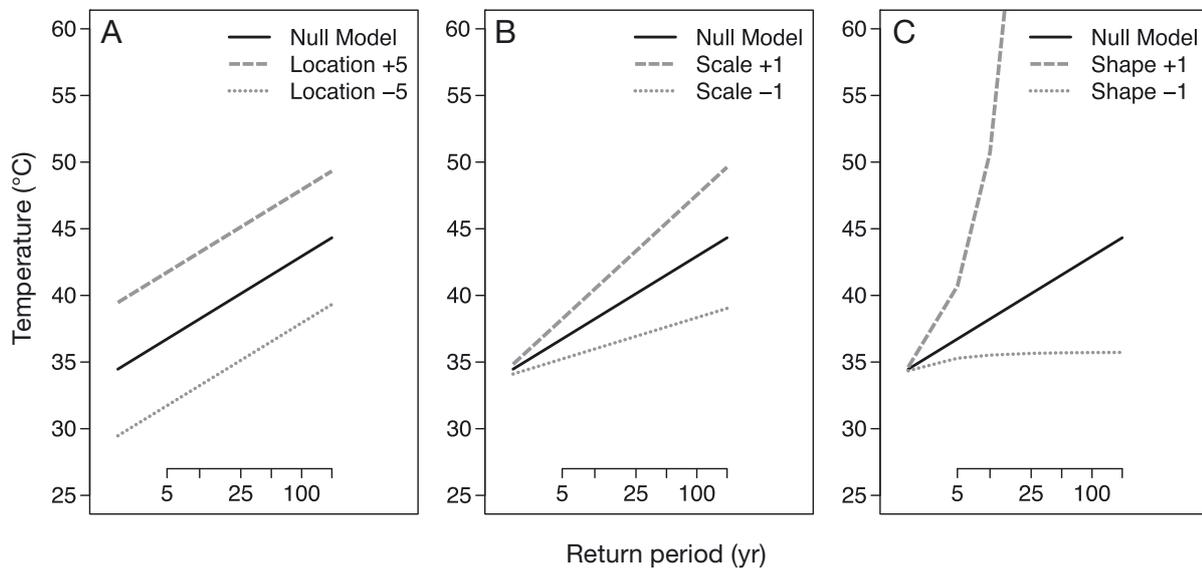

Fig. A2. Return period estimates for the null model (black lines) with parameters $\mu = 34$, $\sigma = 2$ and and $\xi = 0$. The location parameter varied by ±5, the scale parameter by ±1 and the shape parameter by ±1 (dashed lines in A,B,C, respectively)